A drill-string model: deterministic and stochastic analysis

T. G. Ritto [a,b] R. Sampaio [a] C. Soize [b]

[a] *Mechanical Engineering Department – PUC-Rio, Rua Marquês de São Vicente, 225, Gávea, RJ, CEP: 22453-900, Brazil, rsampaio@puc-rio.br, thiagoritto@gmail.com*

[b] *Université Paris-Est, Laboratoire de Modélisation et Simulation Multi Echelle, MSME FRE3160 CNRS, 5 bd Descartes, 77454 Marne-la-Vallée, France, christian.soize@univ-paris-est.fr*

Abstract

A drill-string is a slender structure that turns and drills into the rock in a search of oil, a numerical model is developed using the Timoshenko beam theory and discretized by means of the Finite Element Method. The drill-string dynamics is difficult to predict due to the nonlinearities and uncertainties involved in the problem. The aim of this work is (1) to present a determinist model and (2) to propose a stochastic model of the bit-rock interaction model. The model considers the main efforts that the column is subjected to: rotation at the top; hanging force at the top; bit-rock interaction; fluid-structure interaction (that takes into account the drilling fluid that flows downwards the column then goes upwards the annulus); shock and rubbing between the column and the borehole; finite strains (what couples axial, torsional, and lateral vibrations); and the own weight of the column. Concerning the dynamics of a drill-string, one source of uncertainty, maybe the most important, is the bit-rock interaction. A stochastic model is developed for a bit-rock interaction to take into account uncertainties in it. Based on the Nonparametric Probabilistic Approach and the Maximum Entropy Principle a probability density function is constructed for the bit-rock operator, then Monte Carlo simulations are done to generate the stochastic dynamic responses. This is a new approach to take into account model uncertainties in local nonlinearities using the Nonparametric Probabilistic Approach.

Key words:
drill-string dynamics, nonlinear dynamics, fluid-structure interaction, bit-rock interaction, bit-rock stochastic model, stochastic dynamics, Nonparametric Probabilistic Approach

Conference presented to the I CAIM 2008

1 Introduction

This paper is concerned with: (1) the modeling of the nonlinear drill-string dynamics and (2) stochastic analysis of the problem. We search a continuous model with a good cost-benefit relationship that incorporates the main effects that influence the column dynamics (the inclusion of a fluid-structure interaction model, for example). With this simple, but quite complete, model we are ready to analyzed uncertainties, then a stochastic model of the bit-rock interaction model is proposed. There are some papers in which a nonlinear dynamic model is developed inspired in the drill-string dynamics, e.g. [7, 8, 40, 41, 15, 16, 4, 39, 24, 28]. These models are able to quantify some effects that occur in a drilling operation, as the stick-slip oscillations, for instance, but they cannot predict correctly the dynamic response of a real system. This is explained, first, because the above models are too simple compared to the real system and, second, because the uncertainties are not taken into account. Each author uses a different approach to the problem: [42, 7] use a one-mode approximation to analyze the problem; [15, 16, 24, 28] use the Euler-Bernoulli beam model with the Finite Element Method; while [40, 41] use the Cosserat theory.

A fluid-structure interaction that takes into account the drilling fluid that flows inside and outside the column is not considered in any of the above works. This kind of fluid-structure interaction model was proposed in [21] for a plane problem in another context, and it will be extended here for our problem.

In this work the Timoshenko beam model is employed and the Finite Element Method is used to discretize the system. Besides, it is considered: finite strain with no simplifications (higher order terms are not neglected); quadratic terms derived from the kinetic energy; shock and rubbing between the column and the borehole; stabilizers; fluid-structure interaction; and a bit-rock interaction [41] that models how the bit penetrates the rock. To derive the equations of motion, the Total Lagrangian (TL) formulation is used (the equations are written in the undeformed configuration and in the inertial (non-rotational) frame), six degrees of freedom are considered in the points of discretization (three translations u, v, and w, and three rotations θ_x, θ_y, and θ_z), the stress tensor is the second Piola-Kirchhoff tensor, and finite strains are considered (Green-Lagrange strain tensor). The strategy used in this work is, in some respects, similar to the one used in [16], but there are several important additional features, such as shock and rubbing between the column and the borehole, shear (Timoshenko beam model), finite θ_x, fluid-structure interaction that takes into account the flow downwards inside the column and upwards in the annulus, all the terms of the strain energy are used in the analysis, a bit-rock interaction model that allows the simulation of the bit penetration is used, constant force at the top (hanging force or weight-on-hook, WOH).

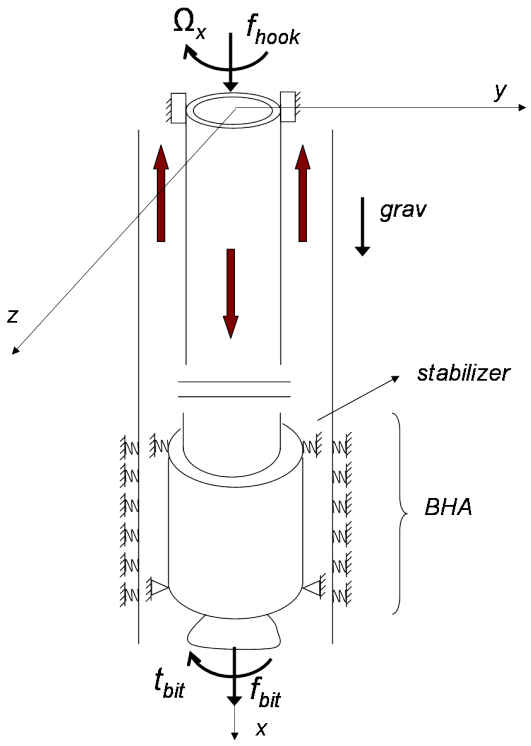

Fig. 1. General scheme.

The drill-string is a slender structure composed by thin tubes called drill-pipes that together have some kilometers (in our simulations 1.4 km) and some thicker tubes called drill-collars that together have some hundred meters (in our simulations 200 m). The region composed by the thicker tubes, called Bore-Hole-Assembly (BHA), is under compression and also subjected to shock and rubbing. That is the reason the tubes are stiffer in the bottom. Figure 1 shows the general scheme of the system analyzed. The imposed forces are: the motor torque (as a constant rotation speed at the top Ω_x); a constant hook force f_{hook}; the torque t_{bit} and force f_{bit} at the bit; the weight of the column; the fluid forces; the shock and rubbing between the column and the borehole; the forces due to the stabilizer; plus the elastic and kinetic forces due to the deformation and to the motion of the structure.

In a drilling operation there are many sources of uncertainties as, for instance: the material properties of the column and the drilling fluid; the dimensions of the system, specially the borehole; the fluid-structure interaction; the bit-rock interaction, among others. This paper is concerned with the stochastic model of the bit-rock interaction because in the opinion of the authors this is one of the most important uncertainties that affect the system response. There are not many articles treating the stochastic problem of the drill-string dynamics, in special we might cite [37, 17]. In [37] lateral forces at the bit are modeled as stochastic, and in [17] the weight-on-bit (wob) is modeled as stochastic in

a simple two degrees of freedom drill-string model. The bit-rock interaction model chosen was the one developed in [41] basically for two reasons: 1) it is able to reproduce the main phenomena (as stick-slip oscillations); 2) it describes well the penetration of the bit into the rock (so we can analyze the rate-of-penetration-ROP). Usually the bit is considered fixed, [16, 24, 28], or an average rate of penetration is assumed, [38, 8].

The probability density function of the bit-rock interaction model operator is derived using the Nonparametric Probabilistic Approach to model uncertainties in mechanical systems [32, 33, 34, 36, 35, 5] which uses the Maximum Entropy Principle [31]. Then two stochastic models are developed: one that allows only parameters to change (called non-coupled model) and another that permits changes in the model (called coupled model). Then by perturbing the bit-rock operator the robustness of the models employed is analyzed.

2 Finite element disctretization

To derive the dynamic equations the extended Hamilton Principle is used ([26, 22]). The first variation of Π must vanish:

$$\delta\Pi = \int_{t_1}^{t_2} (\delta U - \delta T - \delta W) dt = 0\,. \tag{1}$$

where U is the potential strain energy, T is the kinetic energy and W is the work done by the nonconservative forces and any force not accounted in the potential energy. In the discretization by means of the Finite Element Method ([14, 2, 25]), a two-node approximation with six degrees of freedom per node is chosen. The nodal displacement is written as: $u_e = \mathbf{N}_u \mathbf{q}_e$, $v_e = \mathbf{N}_v \mathbf{q}_e$, $w_e = \mathbf{N}_w \mathbf{q}_e$, $\theta_{xe} = \mathbf{N}_{\theta_x} \mathbf{q}_e$, $\theta_{y_e} = \mathbf{N}_{\theta_y} \mathbf{q}_e$, $\theta_{ze} = \mathbf{N}_{\theta_z} \mathbf{q}_e$, where $\mathbf{N}$ are the shape functions (see [19, 3]); u_e, v_e, and w_e are the displacements in x, y, and z directions; θ_{xe}, θ_{ye}, and θ_{ze} are the rotations in x, y, and z axis.$\mathbf{q}_e = \begin{pmatrix} u_1 & v_1 & \theta_{z1} & w_1 & \theta_{y_1} & \theta_{x1} & u_2 & v_2 & \theta_{z2} & w_2 & \theta_{y_2} & \theta_{x2} \end{pmatrix}^T$, where $(\cdot)^T$ means transpose. After assemblage, the final discretized equation is written as

$$([M]+[M_f])\ddot{\mathbf{q}}+([C]+[C_f])\dot{\mathbf{q}}+([K]+[K_f]+[K_g(\mathbf{q})])\mathbf{q} = \mathbf{f}_{NL}(\mathbf{q},\dot{\mathbf{q}},\ddot{\mathbf{q}})+\mathbf{f}_c+\mathbf{f}_g+\mathbf{f}_f\,. \tag{2}$$

The response $\mathbf{q}$ is represented in a subspace $V_m \subset \mathbb{R}^m$, where m equals the number of degrees of freedom of the system. $[M]$, $[C]$, and $[K]$ are the classical mass, damping and stiffness matrices; $[M_f]$, $[C_f]$, $[K_f]$ are the fluid mass, damping and stiffness matrices, and $\mathbf{f}_f$ is the fluid force vector; $[K_g(\mathbf{q})]$ is the geometric stiffness matrix; $\mathbf{f}_g$ is the gravity force; $\mathbf{f}_c$ is a concentrated reaction force at the bit; $\mathbf{f}_{NL}(\mathbf{q},\dot{\mathbf{q}},\ddot{\mathbf{q}})$ is the nonlinear force vector that is decomposed

in four parts as follows,

$$\mathbf{f}_{NL}(\mathbf{q}, \dot{\mathbf{q}}, \ddot{\mathbf{q}}) = \mathbf{f}_{ke}(\ddot{\mathbf{q}}, \dot{\mathbf{q}}, \mathbf{q}) + \mathbf{f}_{se}(\mathbf{q}) + \mathbf{f}_{sh}(\mathbf{q}) + \mathbf{f}_{br}(\dot{\mathbf{q}})\,. \tag{3}$$

where $\mathbf{f}_{ke}(\mathbf{q}, \dot{\mathbf{q}}, \ddot{\mathbf{q}})$ is composed by the quadratic terms of the kinetic energy; $\mathbf{f}_{se}(\mathbf{q})$ is composed by the quadratic and higher order terms of the strain energy; $\mathbf{f}_{sh}(\mathbf{q})$ are the forces due to the shock and rubbing between the column and the borehole; $\mathbf{f}_{br}(\dot{\mathbf{q}})$ are the forces due to the bit-rock interactions.

3 Initial prestressed configuration

Before starting the rotation about x-axis, the column gets down through the channel until it reaches the soil. At this point there are three forces acting: the reaction force at the bit, the weight of the drill-string and the hook force that supports the system. In this equilibrium configuration, the system is prestressed. There is a neutral point: above which the column is under tension and below it the column is under compression.

We consider variations from the initial stressed state which is calculated using $\mathbf{f}_g$ (gravity force) and $\mathbf{f}_c$ (concentrated force at the bit that depends on the weight-on-bit, *wob*):

$$\mathbf{q}_S = [K]^{-1}(\mathbf{f}_g + \mathbf{f}_c)\,. \tag{4}$$

Substituting the above expression in Eq. (2) yields

$$([M]+[M_f])\ddot{\bar{\mathbf{q}}}+([C]+[C_f])\dot{\bar{\mathbf{q}}}+([K]+[K_f]+[K_g(\mathbf{q}_S)])\bar{\mathbf{q}} = \mathbf{f}_{NL}(\bar{\mathbf{q}}, \dot{\bar{\mathbf{q}}}, \ddot{\bar{\mathbf{q}}})+\mathbf{f}_f\,, \tag{5}$$

in which $\bar{\mathbf{q}} = \mathbf{q} - \mathbf{q}_S$.

4 Kinetic energy

The first variation of the kinetic energy is written as

$$\delta T = -\int_0^L \big[\rho A\ddot{u}\delta u + \rho A\ddot{v}\delta v + \rho A\ddot{w}\delta w + \rho I\ddot{\theta}_y\delta\theta_y + \rho I\ddot{\theta}_z\delta\theta_z + \rho I_p\ddot{\theta}_x\delta\theta_x +$$

$$+ (\rho I_p(-\theta_y\ddot{\theta}_z\delta\theta_x - \dot{\theta}_y\dot{\theta}_z\delta\theta_x + \dot{\theta}_x\dot{\theta}_z\delta\theta_y - \dot{\theta}_x\dot{\theta}_y\delta\theta_z - \theta_y\ddot{\theta}_x\delta\theta_z))\Big]\, dx\,. \qquad (6)$$

where ρ is the mass density, A is the cross sectional area, L is the length of the column, $[I_t]$ is the cross sectional inertial matrix, $\mathbf{v}$ is the velocity vector, $\boldsymbol{\omega}$ the angular velocity vector. The three following quantities $\mathbf{v}$, $[I_t]$ and $\boldsymbol{\omega}$ are written as

$$\mathbf{v} = \begin{pmatrix} \dot{u} \\ \dot{v} \\ \dot{w} \end{pmatrix} \quad , \quad [I_t] = \begin{pmatrix} I_p & 0 & 0 \\ 0 & I & 0 \\ 0 & 0 & I \end{pmatrix} \quad , \quad \boldsymbol{\omega} = \begin{pmatrix} \dot{\theta}_x + \theta_y\dot{\theta}_z \\ cos(\theta_x)\dot{\theta}_y - sin(\theta_x)\dot{\theta}_z \\ sin(\theta_x)\dot{\theta}_y + cos(\theta_x)\dot{\theta}_z \end{pmatrix}. \qquad (7)$$

The time derivative is denoted by $da/dt = \dot{a}$. The angular velocity $\boldsymbol{\omega}$ is written in the inertial referential assuming small angles (θ_y and θ_z) and it is derived by first rotating the inertial frame about the x-axis, θ_x, then rotating the resulting frame about the y-axis, θ_y, and finally, rotating the resulting frame about the z-axis, θ_z.

5 Strain energy

The first variation of the strain energy is given by

$$\delta U = \int_V (E\delta\epsilon_{xx}\epsilon_{xx} + 4k_sG\delta\gamma_{xy}\gamma_{xy} + 4k_sG\delta\gamma_{xz}\gamma_{xz})dV\,. \qquad (8)$$

where V is the region of integration, $\boldsymbol{\epsilon} = (\epsilon_{xx} \quad 2\gamma_{xy} \quad 2\gamma_{xz})^T$ is the Green-Lagrange strain tensor.

The Timoshenko beam model is used because the impacts at the bottom and the complex nonlinear dynamics may induce shear, and also because the Timoshenko beam model includes the Euler-Bernoulli model. The displacements written in the undeformed configuration are

$$\begin{aligned} &u_x = u - y\theta_z + z\theta_y \quad , \quad u_y = v + y(\cos(\theta_x) - 1) - z\sin(\theta_x), \\ &u_z = w + z(\cos(\theta_x) - 1) + y\sin(\theta_x)\ , \end{aligned} \qquad (9)$$

in which u, v and w are the displacements of the neutral line. The space derivative is denoted by $da/dx = a'$. Note that θ_x has not been simplified in the above expression. Note also that due to the finite strain formulation, the axial, torsional and lateral vibrations are coupled.

6 shock and rubbing

The forces due to the shocks between the column and the borehole are modeled by concentrated forces and torques at the nodes in the region of the drill-collar. The lateral forces are modeled as an elastic force governed by the stiffness parameter k_{sh} [N/m]. The rubbing between the column and the borehole is simply modeled as a friction torque governed by the friction coefficient μ_{sh}.

7 Bit-rock interaction model

In this work, the model used is the one developed by [41], which is rewritten as

$$f_{xbit} = -\frac{\dot{u}_{bit}}{a_2 Z(\dot{\theta}_{bit})^2} + \frac{a_3 \dot{\theta}_{bit}}{a_2 Z(\dot{\theta}_{bit})} - \frac{a_1}{a_2} \quad , \quad t_{xbit} = -\frac{\dot{u}_{bit} a_4 Z(\dot{\theta}_{bit})^2}{\dot{\theta}_{bit}} - a_5 Z(\dot{\theta}_{bit}) \tag{10}$$

in which f_{xbit} is the axial force, where t_{xbit} is the torque about the x-axis and where $Z(\dot{\theta}_{bit})$ is the regularizing function.

In the above equation, $a_1, \ldots, a_5$ are positive constants that depend on the bit and rock characteristics as well as on the weight-on-bit (wob). This equation was derived for a stable operation with $\dot{\theta}_{bit} \sim 100$ RPM and with $wob \sim 100$ kN.

In this model, the bit exerts only an axial force (f_{xbit}) and a torque (t_{xbit}) about the x-axis. These force and torque exerted by the rock at the bit depend on the axial speed ($\dot{u}_{bit}$) and the rotation speed ($\dot{\theta}_{bit}$) of the bit. Note that these forces at the bit couple axial and torsional vibrations.

8 Fluid

The drilling fluid (mud) is responsible to transport the cuttings (drilled solids) from the bottom to the top to avoid clogging of the hole. It also plays an important role in cooling and stabilizing the system [1]. The rheological properties of the mud are complexes, see [9] for instance. There is no doubt that the drilling fluid influences the dynamics of a drill-string, but to solve the complete problem would be too expensive computationally. There are some works that study only the drilling fluid flow, as, for example, [11, 12, 23]. We decided to use a linear fluid-structure coupling model similar to [20, 21]. In this simplified model there are the following hypotheses,

(1) The inside fluid is inviscid, while the outside flow is viscous.
(2) The flow induced by the rotation speed about x-axis is not considered in this analysis.
(3) The pressure varies linearly with x.
(4) The fluid is added in the formulation as a constant mass matrix $[M_f]$, a constant stiffness matrix $[K_f]$, a constant damping matrix $[C_f]$ and a constant force $\mathbf{f}_f$ (see Eq. (11)).

For a matter of space we will write directly the equations for an element. These equations are an extension and an adaptation of the model developed in [21]. We have,

$$
\begin{aligned}
[M_f]^{(e)} &= \int_0^1 \left(M_f + \chi\rho_f A_o\right)\left(\mathbf{N}_w^T\mathbf{N}_w + \mathbf{N}_v^T\mathbf{N}_v\right) l_e d\xi \,, \text{ (added mass)} \,, \\
[K_f]^{(e)} &= \int_0^1 \left(-M_f U_i^2 - A_i p_i + A_o p_o - \chi\rho_f A_o U_o^2\right)\left(\mathbf{N'}_w^T\mathbf{N'}_w + \mathbf{N'}_v^T\mathbf{N'}_v\right)\frac{1}{l_e} d\xi + \\
&\quad + \int_0^1 \left(-A_i\frac{\partial p_i}{\partial x} + A_o\frac{\partial p_o}{\partial x}\right)\left(\mathbf{N}_{\theta_y}^T\mathbf{N}_{\theta_y} + \mathbf{N}_{\theta_z}^T\mathbf{N}_{\theta_z}\right) l_e d\xi \,, \text{ (added stiffness)} \,, \\
[C_f]^{(e)} &= \int_0^1 \left(-2M_f U_i + 2\chi\rho_f A_o U_o\right)\left(\mathbf{N}_{\theta_y}^T\mathbf{N}_{\theta_y} + \mathbf{N}_{\theta_z}^T\mathbf{N}_{\theta_z}\right) l_e d\xi + \\
&\quad + \int_0^1 \left(\frac{1}{2}C_f\rho_f D_o U_o + k\right)\left(\mathbf{N}_w^T\mathbf{N}_w + \mathbf{N}_v^T\mathbf{N}_v\right) l_e d\xi \,, \text{ (added damping)} \,, \\
\mathbf{f}_f^{(e)} &= \int_0^1 \left(M_f g - A_i\frac{\partial p_i}{\partial x} - \frac{1}{2}C_f\rho_f D_o U_o^2\right)\mathbf{N}_u^T l_e d\xi \,. \text{ (added axial force)} \,,
\end{aligned}
\tag{11}
$$

in which,

M_f is the fluid mass per unit length,
ρ_f is the density of the fluid,
$\chi = \dfrac{(D_{ch}/D_o)^2 + 1}{(D_{ch}/D_o)^2 - 1} \quad (> 1)$,
D_{ch} is the borehole (channel) diameter,
D_i, D_o are the inside and outside diameters of the column,
U_i, U_o are the inlet and outlet flow velocities,
p_i, p_o are the pressures inside and outside the drill-string,
A_i, A_o are the inside and outside cross sectional area of the column,
C_f, k are the fluid viscous damping coefficients.

It is assumed that the inner and the outer pressures (p_i and p_o) vary linearly with x and are then written as

$$p_i = (\rho_f g+)\, x + p_{cte}\,, \tag{12}$$

$$p_o = \left(\rho_f g + \frac{F_{fo}}{A_o}\right) x\,, \tag{13}$$

where p_{cte} is a constant pressure and where F_{fo} is the friction forces due the outside flow given by

$$F_{fo} = \frac{1}{2} C_f \rho_f \frac{D_o^2 U_o^2}{D_h}\,. \tag{14}$$

In the above equation, D_h is the hydraulic diameter ($=4A_{ch}/S_{tot}$) and S_{tot} is the total wetted area per unit length ($\pi D_{ch} + \pi D_o$).

Note that the reference pressure is $p_o(x = 0) = 0$. Another assumption is that there is no head loss when the fluid passes from the drill-pipe to the drill-collar (and vice-versa). The head loss due to the change in velocity of the fluid at the bottom (it was going down, then it goes up) is given by

$$h = \frac{1}{2g}(U_i - U_o)^2\,. \tag{15}$$

In [21] this expression is derived for a column free at the bottom, which is not the case here. Nevertheless in this work we will not change this expression because the simulations showed that, even if h is multiplied by ten, the results do not change significantly.

Note that if the geometry and the fluid characteristics are given, we can only control the inlet flow velocity $U_i(x = 0)$ because the outlet velocity is calculated using the continuity equation and the pressures are calculated using the Bernoulli equation.

Examining Eq. (11), it can be seen that the mass matrix due to the fluid is the usual added mass that, in our case, represents a significative value. For example, using representative values (used in our simulations), the added mass is around 50%, what changes the natural frequencies in about 20%.

The stiffness matrix due to the fluid depends on the speed of the inside and outside flow, on the pressure and on the pressure derivatives. Analyzing the signs in the equation (Eq. 11) we see that the outsize pressure tends to stabilize the system while the inside pressure and the flow tends to destabilize the system. The term $(-p_i A_i + p_o A_0)$ plays a major role on the stiffness of the system because, even though p_i is close to p_o, in the drill collar region (in

the bottom) A_0 is around ten times A_i what turns the system stiffer at the bottom, see Section 13.1.

The damping matrix due to the fluid depends on the flow velocity as well as in the viscous parameter of the fluid, which are not well established values. There are uncertainties to determine the damping characteristics and a stochastic model should be developed to the damping, but in this work a detailed analysis will not be addressed.

Finally, the force vector ($\mathbf{f}_f$) represents the buoyancy induced by the fluid and it is the only force in the axial direction (x-direction).

9 Boundary and initial conditions

As boundary conditions it is considered that at the top ($x = 0$) there are no transversal displacements ($v = w = 0$), the rotations about y and z-axis are zero ($\theta_y = \theta_z = 0$), and a constant rotation speed about x-axis is imposed: $\theta_x(x = 0) = \Omega_x$. At the bit ($x = L$) there are no transversal displacements ($v = w = 0$).

In drilling operations there are stabilizers in the BHA region that turn the system stiffer and help to diminish the amplitude of the lateral vibrations. Stabilizers are considered as an elastic element at the point separating the drill-pipes from the drill-collars: $F_y(x = stab) = k_{stab}\, v(x = stab)$ and $F_z(x = stab) = k_{stab} w(x = stab)$, where $stab$ means stabilizer.

To apply the boundary conditions above, the lines and rows corresponding to $v|_{x=0}$, $v|_{x=L}$, $w|_{x=0}$, $w|_{x=L}$, $\theta_y|_{x=0}$, $\theta_z|_{x=0}$, and $\theta_x|_{x=0}$ of the full matrices ($[M]$, $[C]$ and $[K]$) are eliminated and the corresponding forces of the imposed velocity at the top (Ω_x) is considered in the right side of the equation.

For the initial condition in time it is assumed that $\theta_x(t = 0) = 100$ RPM and that $u(t = 0)$=15 m/h, so the system starts with two rigid motions.

10 Reduced model: choice of the reduction basis

Usually the final discretized FE system have big matrices (dimension $m \times m$) and the dynamic analysis may be time consuming, which is the case of the analysis presented herein. A possible method for nonlinear dynamical systems (see for instance [10, 32, 29]) is to project the nonlinear dynamical equation on a subspace $V_n \in \mathbb{R}^m$, with $n << m$, spanned by a basis related to the

dynamics that is able to represent the system in this subspace. There are several possibilities for this choice, POD/Karhunen-Loève could be one of them, [39, 27].

In this paper, the basis used for the reduction corresponds to the normal modes projection, but, as it will be pointed out later, these normal modes have to properly be chosen (they can not be taken simply in the order that they appear). The normal modes are calculated with $[M]$ and $([K]+[K_g(\mathbf{q}_S)])$ solving the following generalized eigenvalue problem,

$$(-[M]\omega^2 + ([K] + [K_g(\mathbf{q}_S)]))\boldsymbol{\phi} = \mathbf{0}\,, \tag{16}$$

where $\boldsymbol{\phi}_i$ is the i-th normal mode and ω_i is the i-th natural frequency. Note: if the fluid is taken into account the normal modes are calculated with $([M]+[M_f])$ and $([K]+[K_f]+[K_g(\mathbf{q}_S)])$.

Using the representation

$$\overline{\mathbf{q}}(t) = [\Phi]\,\mathbf{a}(t)\,, \tag{17}$$

and substituting it in the equation of motion yield

$$[M][\Phi]\ddot{\mathbf{a}} + [C][\Phi]\dot{\mathbf{a}} + ([K] + [K_g(\mathbf{q}_S)])[\Phi]\mathbf{a} = \mathbf{f}_{NL}(\bar{\mathbf{q}}, \dot{\bar{\mathbf{q}}}, \ddot{\bar{\mathbf{q}}})\,. \tag{18}$$

where $[\Phi]$ is a $(m \times n)$ real matrix composed by n normal modes. Projecting the equation on the subspace spanned by these normal modes yields

$$[\Phi]^T[M][\Phi]\ddot{\mathbf{a}} + [\Phi]^T[C][\Phi]\dot{\mathbf{a}} + [\Phi]^T([K] + [K_g(\mathbf{q}_S)])[\Phi]\mathbf{a} = [\Phi]^T\mathbf{f}_{NL}(\bar{\mathbf{q}}, \dot{\bar{\mathbf{q}}}, \ddot{\bar{\mathbf{q}}})\,, \tag{19}$$

which can be rewritten as

$$[M_r]\,\ddot{\mathbf{a}}(t) + [C_r]\,\dot{\mathbf{a}}(t) + [K_r]\,\mathbf{a}(t) = [\Phi]^T\mathbf{f}_{NL}(\bar{\mathbf{q}}, \dot{\bar{\mathbf{q}}}, \ddot{\bar{\mathbf{q}}})\,, \tag{20}$$

in which

$$\begin{gathered}[M_r] = [\Phi]^T[M][\Phi], \quad [C_r] = [\Phi]^T[C][\Phi] \\ [K_r] = [\Phi]^T([K] + [K_g(\mathbf{q}_S)])[\Phi]\end{gathered} \tag{21}$$

are the reduced matrices. In the application, the system will be discretized in 56 finite elements, so the number of d.o.f = $57 \times 6 = 342$. For the dynamic response, 32 normal modes is then necessary to reach convergence, i.e. 10 % of the DOF.

11 Damping

The damping of the system is modeled as a viscous damping with matrix $[C] = \alpha[M] + \beta([K] + [K_g(\mathbf{q}_S)])$ (where α and β are constants). Since we need

to construct the reduced damping matrix, we will not effectively construct the damping matrix $[C]$. Instead we will select a damping factor ξ_i for each i-th normal mode normalized with respect to the mass matrix. The reduced damping matrix $[C_r]$ can then be written as

$$[C_r] = \begin{pmatrix} c_1 & 0 & 0 & 0 \\ 0 & c_2 & 0 & 0 \\ 0 & 0 & 2\xi_3\omega_3 & 0 \\ 0 & 0 & 0 & ... \end{pmatrix} . \tag{22}$$

where ω_i and ξ_i are the natural frequency and the damping rate related to the i-th normal mode. Note that in our analysis, the first two natural frequencies are zero due to the rigid body motion, so, these two parameters c_1 and c_2 will control how the rigid body motions lose energy due to friction in time.

12 Stochastic model of the bit-rock interaction model

The Parametric Probabilistic Approach allows physical parameter uncertainties to be modeled [13, 32]. It should be noted that the underlying deterministic model defined by Eq. (10) exhibits parameters (a_1, a_2, a_3, a_4 and a_5) which are obtained by an identification process, so it would be difficult to propose a stochastic model for each one, moreover they are not independent from each other. We then proposed to use the Nonparametric Probabilistic Approach of uncertainties consisting in globally modeling the operator of the constitutive equation, Eq. (10), by a random operator using the approach of [32, 33, 34, 36, 35, 5].

In the early works, the Nonparametric Probabilistic Approach was applied for linear operators [32, 33, 36, 35, 6]. Recently is was extended to nonlinear system [18], but the type of problem studied here is completely different from the geometrically nonlinear dynamical system studied in [18]. We are dealing with a nonlinear operator that is an interaction model (bit-rock interaction), therefore it requires a different methodology, nevertheless we will proceed using the same rational used in the works of C. Soize.

For convenience Eq. (10) is rewritten in a matrix form as

$$\mathbb{F}_{bit}(\dot{\mathbf{x}}) = -[A_b(\dot{\mathbf{x}})]\dot{\mathbf{x}}\,, \tag{23}$$

in which $[A_b(\dot{\mathbf{x}})]$ is the positive-definite matrix depict by:

$$[A_b(\dot{\mathbf{x}})] = \begin{pmatrix} \left(\dfrac{a_1}{a_2\dot{u}_{bit}} + \dfrac{1}{a_2 Z(\dot{\theta}_{bit})^2} - \dfrac{a_3\dot{\theta}_{bit}}{a_2 Z(\dot{\theta}_{bit})\dot{u}_{bit}}\right) & 0 \\ 0 & \left(\dfrac{a_4 Z(\dot{\theta}_{bit})^2\dot{u}_{bit}}{\dot{\theta}_{bit}^2} + \dfrac{a_5 Z(\dot{\theta}_{bit})}{\dot{\theta}_{bit}}\right) \end{pmatrix}, \tag{24}$$

and

$$\mathbb{F}_{bit}(\dot{\mathbf{x}}) = \begin{pmatrix} f_{bit} \\ t_{bit} \end{pmatrix} \quad \text{and} \quad \dot{\mathbf{x}} = \begin{pmatrix} \dot{u}_{bit} \\ \dot{\theta}_{bit} \end{pmatrix}.$$

The final form of $[A_b(\dot{\mathbf{x}})]$ is not obvious, but analyzing the virtual power of the system which can be written as:

$$\delta\mathcal{P}_{bit}(\dot{\mathbf{x}}) = \quad < \mathbb{F}_{bit}(\dot{\mathbf{x}}), \delta\dot{\mathbf{x}} > \quad = \quad < -[A_b(\dot{\mathbf{x}})]\dot{\mathbf{x}}, \delta\dot{\mathbf{x}} > . \tag{25}$$

Then we see that to recover the force $\mathbb{F}_{bit}(\dot{\mathbf{x}})$ one should do:

$$\mathbb{F}_{bit}(\dot{\mathbf{x}}) = \nabla_{\delta\dot{\mathbf{x}}}\ \delta\mathcal{P}_{bit}(\dot{\mathbf{x}})\,, \tag{26}$$

$$\mathbb{F}_{bit}(\dot{\mathbf{x}}) = -[A_b(\dot{\mathbf{x}})]\dot{\mathbf{x}} = -\begin{pmatrix} \dfrac{a_1}{a_2} + \dfrac{\dot{u}_{bit}}{a_2 Z(\dot{\theta}_{bit})^2} - \dfrac{a_3\dot{\theta}_{bit}}{a_2 Z(\dot{\theta}_{bit})} \\ \dfrac{a_4 Z(\dot{\theta}_{bit})^2\dot{u}_{bit}}{\dot{\theta}_{bit}} + a_5 Z(\dot{\theta}_{bit}) \end{pmatrix}. \tag{27}$$

To verify the positive-definiteness of $[A_b(\dot{\mathbf{x}})]$, we simply check if the diagonal terms are greater than zero. This is true for the range of values that we are working with.

The Nonparametric Probabilistic Approach consists, for all deterministic vector $\dot{\mathbf{x}}$, in modeling the matrix $[A_b(\dot{\mathbf{x}})]$ by a random matrix $[\mathbf{A}_b(\dot{\mathbf{x}})]$ with values in the set $\mathbb{M}_n^+(\mathbb{R})$, with $n = 2$, of all the positive-definite symmetric $(n \times n)$ real matrices. Note that for each time the matrix $[\mathbf{A}_b(\dot{\mathbf{x}})]$ will be different because it depends on $\dot{\mathbf{x}}$ that changes with time, but this will not impose any problem for the strategy that will be adopted.

In order to apply the Nonparametric Probabilistic Approach for the operator $[A_b(\dot{\mathbf{x}})]$, we have to define the available information and in a second step

construct the probability density function of the random matrix using the Maximum Entropy Principle. The available information is made up of

(1) $\forall\ \dot{\mathbf{x}}$, random matrix $[\mathbf{A}_b(\dot{\mathbf{x}})]$ is positive definite almost surely,
(2) $E\{[\mathbf{A}_b(\dot{\mathbf{x}})]\} = [A_b(\dot{\mathbf{x}})]$,
(3) $E\{||[\mathbf{A}_b(\dot{\mathbf{x}})]^{-1}||_F^2\} = \text{constant}_1 < +\infty$,

in which $E\{\cdot\}$ is the mathematical expectation, where $|||[B]|||_F$ denotes the Frobenius norm of the matrix $[B]$ and where $[A_b(\dot{\mathbf{x}})]$ is the operator of the mean model. Condition (1) implies that the operator is invertible almost surely. Condition (3) implies that Eq. (23) can be inverse in the mean-square sense. Following the methodology of the Nonparametric Probabilistic Approach, the mean value is written, using the Cholesky decomposition, as

$$[A_b(\dot{\mathbf{x}})] = [L_b(\dot{\mathbf{x}})]^T [L_b(\dot{\mathbf{x}})]\,, \tag{28}$$

and the random matrix $[\mathbf{A}_b(\dot{\mathbf{x}})]$ is defined by

$$[\mathbf{A}_b(\dot{\mathbf{x}})] = [L_b(\dot{\mathbf{x}})]^T [\mathbf{G}_b][L_b(\dot{\mathbf{x}})]\,. \tag{29}$$

In the above equation, $[\mathbf{G}_b]$ is a random matrix satisfying the following available information,

(1) random matrix $[\mathbf{G}_b]$ is positive definite almost surely,
(2) $E\{[\mathbf{G}_b]\} = [I]$,
(3) $E\{||[\mathbf{G}_b]^{-1}||_F^2\} = \text{constant}_2 < +\infty$,

in which $[I]$ is the unity matrix. It should be noted that, in such a construction, the random matrix $[\mathbf{G}_b]$ does not depend on $\dot{\mathbf{x}}$ nor on time. Taking into account the available information and applying the Maximum Entropy Principle yield an explicit expression [33] of the probability density function $P_{[\mathbf{G}_b]}$ which is written as

$$p_{[\mathbf{G}_b]}([G_b]) = \mathbb{1}_{\mathbb{M}_n^+(\mathbb{R})}([G_b]) C_{\mathbf{G}_b} det([G_b])^{(n+1)\frac{(1-\delta^2)}{2\delta^2}} \exp\left\{-\frac{(n+1)}{2\delta^2} tr[G_b]\right\}, \tag{30}$$

in which $det(\cdot)$ is the matrix determinant, $tr(\cdot)$ is the matrix trace, δ is the dispersion parameter of the distribution and n is the size of random matrix $[\mathbf{G}_b]$ ($n = 2$ in the present case). The constant of normalization is written as

$$C_{\mathbf{G}_b} = \frac{(2\pi)^{-n(n-1)/4} \left(\frac{n+1}{2\delta^2}\right)^{n(n+1)(2\delta^2)^{-1}}}{\left\{\prod_{j=1}^n \Gamma\left(\frac{n+1}{2\delta^2} + \frac{1-j}{2}\right)\right\}}\,, \tag{31}$$

where $\Gamma(z)$ is the gamma function defined for $z > 0$ by $\Gamma(z) = \int_0^{+\infty} t^{z-1} e^{-t} dt$

and where the dispersion parameter δ is given by

$$\delta = \left\{ \frac{1}{n} E\{ ||[\mathbf{G_b}] - [I]||_F^2 \} \right\}^{\frac{1}{2}} , \tag{32}$$

which has to be such that and $0 < \delta < ((n+1)/(n+5))^{1/2}$.

The random generator of independent realizations of random matrix $[\mathbf{G}_b]$, for which the probability density function is defined by Eq. (30), is constructed using the following algebraic representation of random matrix $[\mathbf{G}_b]$ (see [33]). Random matrix $[\mathbf{G}_b]$ can be written as $[\mathbf{G}_b] = [\mathbf{L}_{G_b}]^T [\mathbf{L}_{G_b}]$ in which $[\mathbf{L}_{G_b}]$ is an upper triangular real random matrix such that

(1) The random variables $\{[\mathbf{L}_{G_b}]_{jj'}, j \leq j'\}$ are independents.
(2) For $j < j'$ the real-valued random variable $[\mathbf{L}_{G_b}]_{jj'} = \sigma V_{jj'}$, in which $\sigma = \delta(n+1)^{-1/2}$ and $V_{jj'}$ is a real-valued gaussian random variable with zero mean and unit variance.
(3) For $j = j'$ the real-valued random variable $[\mathbf{L}_{G_b}]_{jj} = \sigma(2V_j)^{1/2}$. In which V_j is a real-valued gamma random variable whose probability density function is written as
$p_{V_j}(v) = \mathbb{1}_{\mathbb{R}^+}(v) \, \frac{1}{\Gamma\left(\frac{n+1}{2\delta^2} + \frac{1-j}{2}\right)} \, v^{\frac{n+1}{2\delta^2} - \frac{1+j}{2}} \, e^{-v}$.

Attention with the stochastic solver because while matrix $[A_b(\dot{\mathbf{x}})]$ changes with time, random matrix $[\mathbf{G}_b]$ is constant in time. In the deterministic equation, we have

$$\mathcal{L}_{NL}(\mathbf{q}(t), \dot{\mathbf{q}}(t), \ddot{\mathbf{q}}(t)) = \mathbf{f}_{bit}(\dot{u}_{bit}(t), \dot{\theta}_{bit}(t)) \, , \tag{33}$$

where $\mathcal{L}_{NL}$ represents all the terms in Eq. (5) except the bit forces. For the stochastic equation, we have

$$\mathcal{L}_{NL}(\mathbf{Q}(t), \dot{\mathbf{Q}}(t), \ddot{\mathbf{Q}}(t)) = \mathbf{F}_{bit}(\dot{U}_{bit}(t), \dot{\Theta}_{bit}(t)) \, , \tag{34}$$

where $\mathbf{Q}(t)$, $\dot{U}_{bit}(t)$, and $\dot{\Theta}_{bit}(t)$ (in capital letters) represent stochastic processes and where, for all fixed $\dot{\mathbf{x}}$, the random force $\mathbf{F}_{bit}(\dot{\mathbf{x}})$ modeling $\mathbb{F}_{bit}(\dot{\mathbf{x}})$ is written as

$$\mathbf{F}_{bit}(\dot{\mathbf{x}}) = -[\mathbf{A}_b(\dot{\mathbf{x}})]\dot{\mathbf{x}} \, . \tag{35}$$

Let

$$[\mathbf{G}_b(s_1)], \ldots, [\mathbf{G}_b(s_\nu)] \tag{36}$$

be ν independent realizations of random matrix $[\mathbf{G}_b]$. For each realization s_j, we have to solve the deterministic equation

$$\mathcal{L}_{NL}(\mathbf{Q}(t, s_j), \dot{\mathbf{Q}}(t, s_j), \ddot{\mathbf{Q}}(t, s_j)) = \mathbf{F}_{bit}(\dot{U}_{bit}(t, s_j), \dot{\Theta}_{bit}(t, s_j)) \, . \tag{37}$$

Two stochastic models are then analyzed.

(1) Coupled Nonparametric Probabilistic Model

What is called here the coupled model is the Nonparametric Probabilistic Model where we consider the model uncertainties of the bit-rock interaction model by directly randomizing the matrix $[A_b(\dot{\mathbf{x}})]$. As we have explained above, the deterministic function

$$(\dot{u}_{bit}(t), \dot{\theta}_{bit}(t)) \mapsto [A_b(\dot{u}_{bit}(t), \dot{\theta}_{bit}(t))] \tag{38}$$

is modeled by the random function $(\dot{u}_{bit}(t), \dot{\theta}_{bit}(t)) \mapsto [\mathbf{A}_b(\dot{u}_{bit}(t), \dot{\theta}_{bit}(t))]$ such that (see Eq. (29))

$$[\mathbf{A}_b(\dot{u}_{bit}(t), \dot{\theta}_{bit}(t))] = [L_b(\dot{u}_{bit}(t), \dot{\theta}_{bit}(t))]^T [\mathbf{G}_b][L_b(\dot{u}_{bit}(t), \dot{\theta}_{bit}(t))] \tag{39}$$

and the random force is then given by

$$\mathbf{F}_{bit}(\dot{u}_{bit}(t), \dot{\theta}_{bit}(t)) = [\mathbf{A}_b(\dot{u}_{bit}(t), \dot{\theta}_{bit}(t))] \begin{pmatrix} \dot{u}_{bit}(t) \\ \dot{\theta}_{bit}(t) \end{pmatrix} . \tag{40}$$

This model is called Coupled Nonparametric Probabilistic Model because it introduces an extra coupling in the model:

$$[\mathbf{G}_b] = \begin{pmatrix} [\mathbf{G}_b]_{11} & \zeta \\ \zeta & [\mathbf{G}_b]_{22} \end{pmatrix} \tag{41}$$

where ζ is a stochastic perturbation ($\zeta = [\mathbf{G}_b]_{21} = [\mathbf{G}_b]_{12}$).

(2) Non-coupled Nonparametric Probabilistic Model

What is called here the non-coupled model is the previously model without the extra coupling terms that appear in the extra-diagonal elements ($\zeta = 0$). The idea is not to randomize all the operator, but to see how a global change in the parameters affects the system response. To do so we simply set the extra-diagonal terms of $[\mathbf{G}_b]$ equal to zero,

$$[\mathbf{G}_b] = \begin{pmatrix} [\mathbf{G}_b]_{11} & 0 \\ 0 & [\mathbf{G}_b]_{22} \end{pmatrix} . \tag{42}$$

Like this, there is no extra coupling between $\dot{u}_{bit}$ and $\dot{\theta}_{bit}$. Note that even in the deterministic system $\dot{u}_{bit}$ depends on $\dot{\theta}_{bit}$ and vice-versa.

13 Numerical results

The drill-string was discretized using 56 finite elements. For the dynamics analysis it was used 10 lateral modes, 10 torsional modes, 10 axial modes, and also the two rigid body modes of the structure (axial and torsional). So matrix $[\Phi]$ is composed by 32 modes. This number was chosen after several experiments. Using more modes the response of the system do not change significantly. The system parameters used are representative values that are found in the literature [8, 41, 16, 24], see appendix A.

13.1 Influence of the fluid

Fig. 2 shows a comparison of the dynamic response with and without the fluid-structure interaction mode.

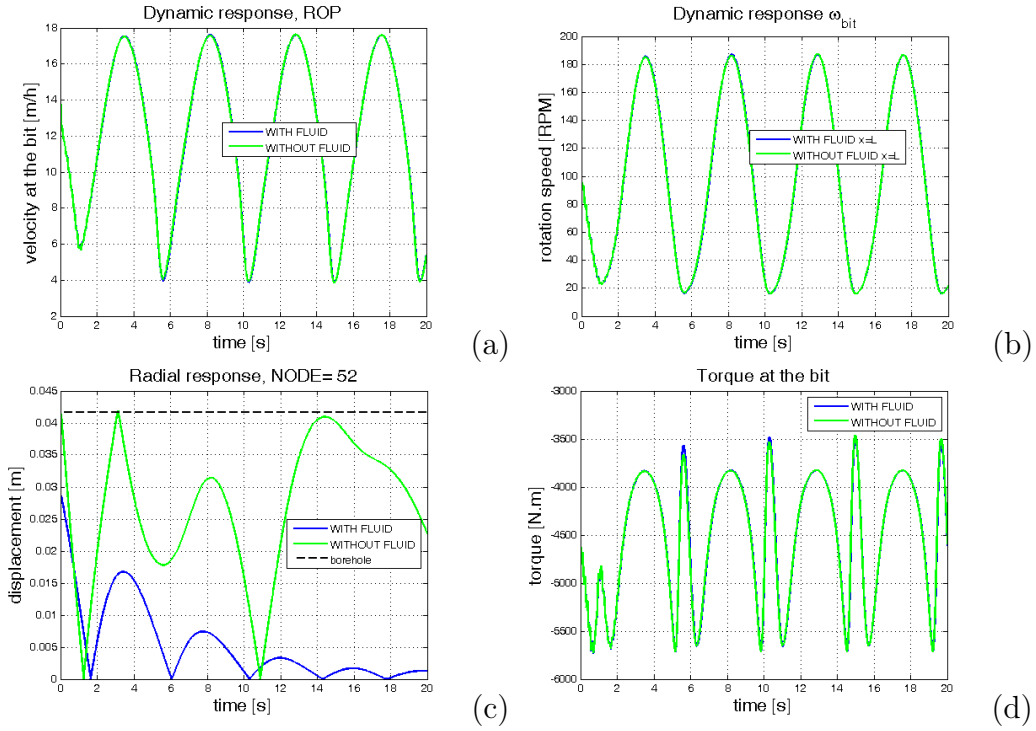

Fig. 2. Response with fluid × without fluid. (a) axial speed at $x = L$, or rate of penetration (ROP); (b) rotation speed at $x = L$ (ω_{bit}); (c) radial displacement at $x = 1560$ m; and (d) torque at the bit.

See in Fig. 2 that the main difference in the dynamic response with and without the fluid-structure interaction model is in the lateral dynamic response, Fig. 2(c). The model used for the fluid has a major influence in the lateral frequencies and lateral mode shapes, see Table 1, but the axial and torsional

frequencies are unaffected, which is not a surprise since in the formulation used (see Section 8) the axial movement is only affected by a constant force $\mathbf{f}_f$, Eq. (11).

Frequency number	Lateral natural freq. (no fluid) (Hz)	Lateral natural freq. (with fluid) (Hz)	Difference (%)
1	0.0287	0.0372	22.8495
2	0.0287	0.0372	22.8495
3	0.0464	0.0744	37.6344
4	0.0464	0.0744	37.6344
5	0.0928	0.1065	12.8638
6	0.0928	0.1065	12.8638
7	0.1098	0.1117	1.7010
8	0.1098	0.1117	1.7010
9	0.1394	0.1488	6.3172
10	0.1394	0.1488	6.3172

Table 1
Natural frequencies with and without fluid

Fig. 3 shows the first lateral mode shapes with and without fluid. Note that because of the presence of the fluid the column is stiffer in the bottom (see the first lateral mode, for instance). This effects occurs mainly due to the term $(p_i A_i + p_o A_o)$ where A_o is around ten times A_i.

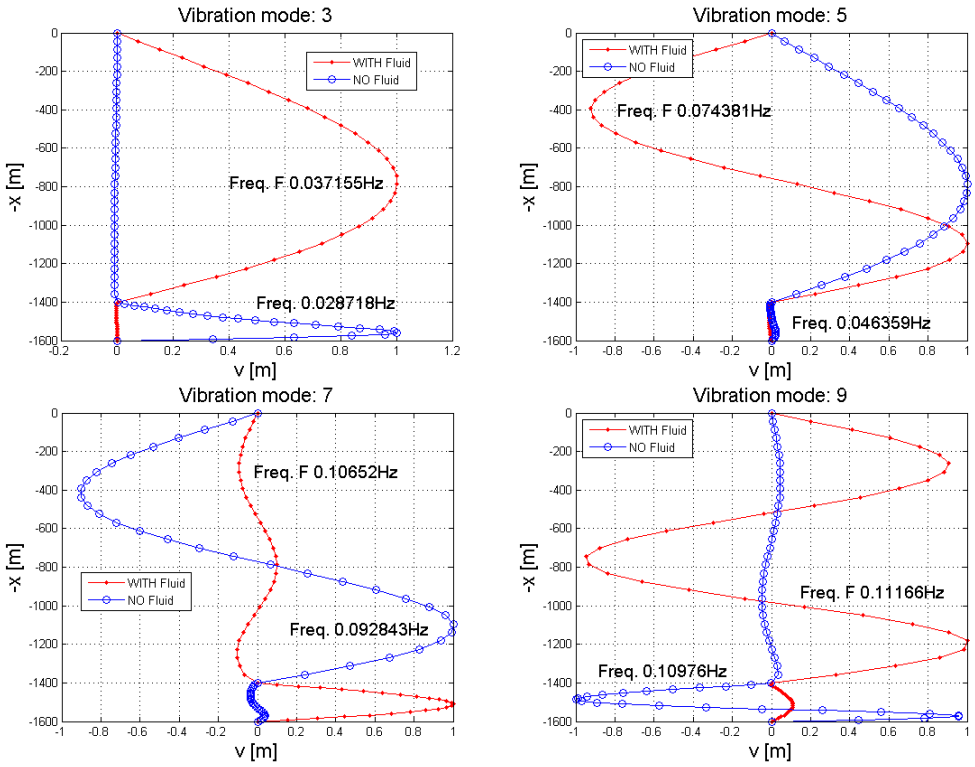

Fig. 3. First lateral mode shapes with and without fluid.

13.2 Considering $\mathbf{f}_{ke} = \mathbf{f}_{se} = 0$

Fig. 4 shows the comparison of the complete dynamics (*case 1*) and the dynamics with $\mathbf{f}_{ke} = \mathbf{f}_{se} = 0$ (*case 2*).

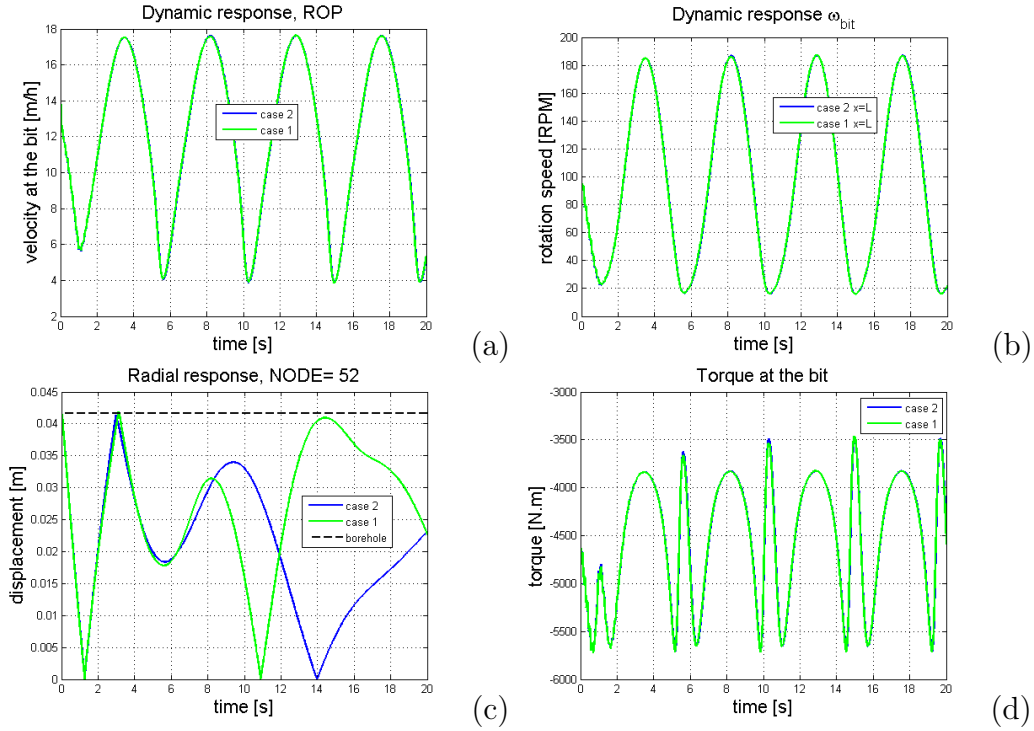

Fig. 4. *Case 1* $\times$ *case 2*. (a) axial speed at $x = L$, or rate of penetration (ROP); (b) rotation speed at $x = L$ (ω_{bit}); (c) radial displacement at $x = 1560$ m; and (d) torque at the bit.

The nonlinear forces $\mathbf{f}_{ke}$ and $\mathbf{f}_{se}$ are important to the dynamic response of the system (take a look at the radial displacement, Fig. 4 (c)), but the torsional and axial displacements are not very affected when $\mathbf{f}_{ke} = \mathbf{f}_{se} = 0$. In fact the simulations showed that $\mathbf{f}_{se}$ is very significant while $\mathbf{f}_{ke}$ is negligible for the case analyzed. We can see that the torsional and axial displacements are mainly dictated by the bit-rock interaction model. Moreover, the time to perform the numerical simulation is around: 70 minutes for *case 1*; and 80 seconds for *case 2*.

As we want to investigate the influence of the probabilistic model of the bit-rock interaction model (axial-torsional nonlinearity) we will use *case 2* for the next simulations, knowing that it is an approximation of the problem analyzed.

13.3 Convergence of the stochastic solution

Let $[\mathbf{U}(t, s)]$ be the response of the stochastic dynamical system calculated for each realization s. The mean-square convergence analysis with respect to the number n_s of independent realizations is carried out studying the function

$n_s \mapsto \mathrm{conv}(n_s)$ defined by

$$\mathrm{conv}(n_s) = \frac{1}{n_s} \sum_{j=1}^{n_s} \int_0^{t_f} ||\mathbf{U}_j(s,t)||^2 dt \,. \tag{43}$$

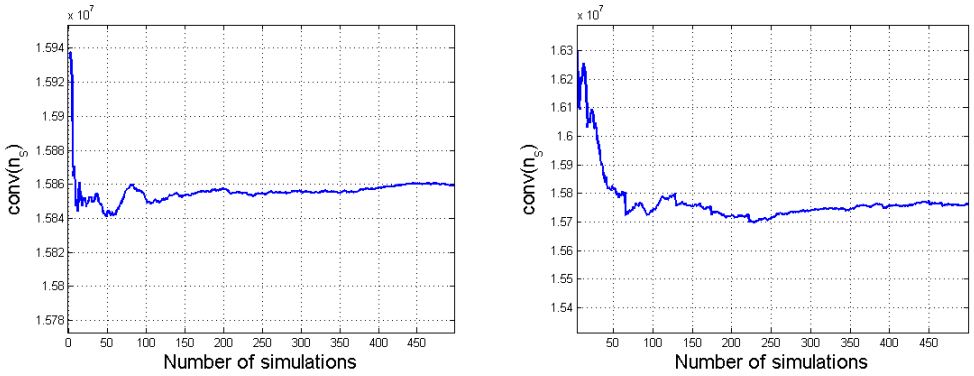

Fig. 5. Convergence of the mean square error for $\delta = 0.1$. Left: coupled model, right: non-coupled model.

Fig. 5 shows that 500 simulations are sufficient to reach the mean-square convergence.

14 Response of the stochastic system

14.1 Non-coupled stochastic model

Fig. 6 shows the 95% envelope (that is to say the confidence region constructed with a probability level of 0.95) for the rotation speed of the bit of the non-coupled stochastic model and for a small dispersion parameter such that $\delta = 0.01$. The envelopes (the upper and lower envelopes of the confidence region) are calculated using the method of quantiles [30].

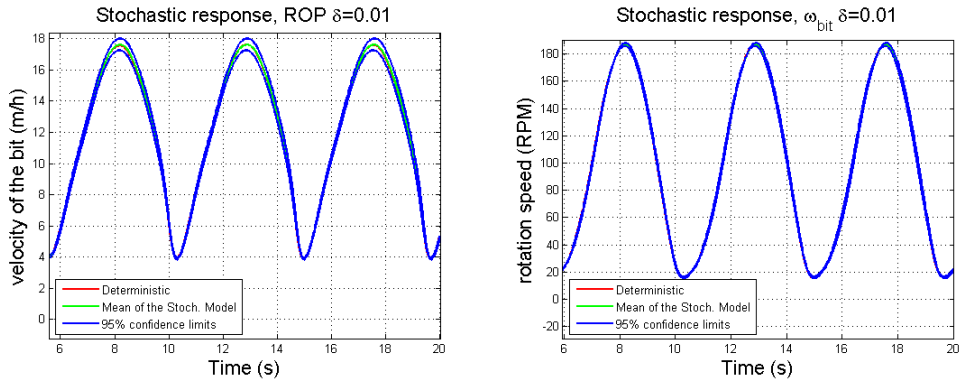

Fig. 6. Non-coupled stochastic model, 95% envelope. Left: rate-of-penetration, ROP. Right: rotation speed of the bit.

We are plotting two important variables: the rate of penetration (ROP) and the rotation speed at the bit (ω_{bit}). So we analyze the influence of the random bit-rock interaction operator in the system response. Fig. 7 shows the stochastic response of the torque at the bit.

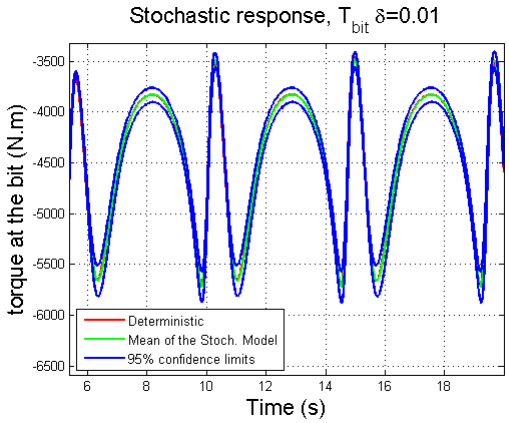

Fig. 7. Non-coupled stochastic model, 95% envelope of the torque at the bit.

It is noted that for $\delta = 0.01$, using the non-coupled stochastic model, the response does not change much, therefore δ will be increased in the next analysis. Fig. 8 to 9 shows the 95% envelope using the non-coupled stochastic model for increasing δ $(= 0.05; 0.2)$.

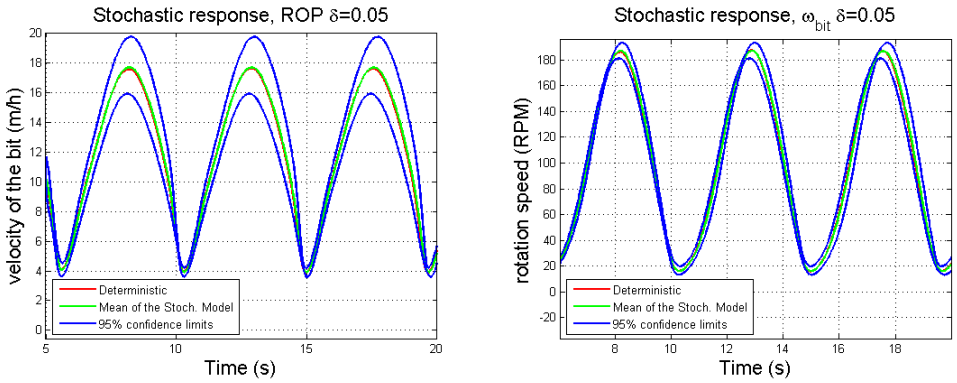

Fig. 8. Non-coupled stochastic model, 95% envelope. Left: rate-of-penetration, ROP. Right: rotation speed of the bit.

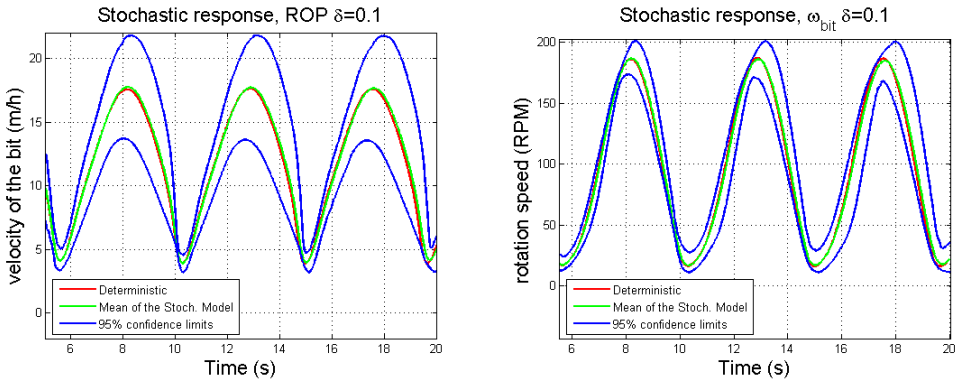

Fig. 9. Non-coupled stochastic model, 95% envelope. Left: rate-of-penetration, ROP. Right: rotation speed of the bit.

As expected, as δ increases the envelope of the response gets wider. Note that the response of the mean model (red line) is almost coincident with the mean response of the stochastic model (green line). In the deterministic analysis the average ROP was around 11 m/h, but now we see that the average ROP can vary from 6 to 16 m/h, which is a significant difference. The variation in rotation speed of the bit should also be analyzed because depending on the response it can cause a system damage. Even if we want to maximize the ROP we do not want the system to collapse.

Another point worth to notice is that as time increases the envelope of the response gets wider (see Fig. 9 right, for example). So, even a small perturbation can cause a great variance on the dynamic response after some time. We also see that the dispersion is greater in the ROP than in ω_{bit}. Fig. 10 shows the 500 Monte Carlo simulations for $\delta = 0.2$.

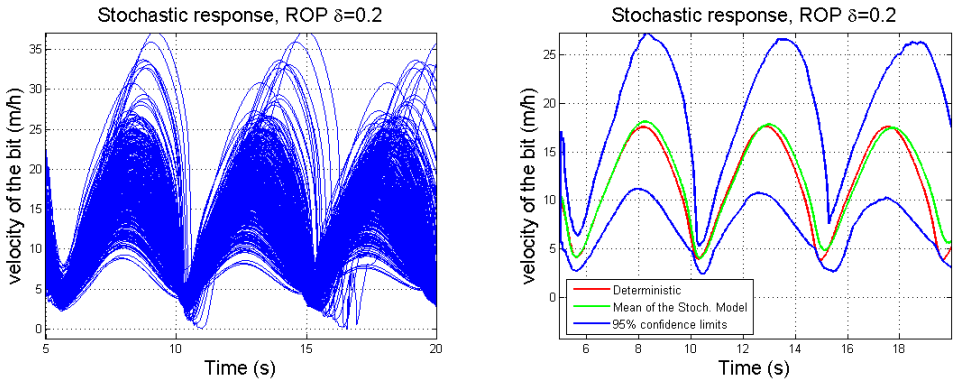

Fig. 10. Non-coupled stochastic model. Left: stochastic responses of the ROP. Right: 95% envelope.

We may say that the bit-rock model used is robust for changes in the parameters because the response seams to be coherent even for $\delta = 0.2$. So this model can be used for different rock properties, or for different cutting characteristics of the bit, for instance.

14.2 Coupled stochastic model

Now lets analyze the results using the coupled stochastic model. Fig. 11 shows the 95% envelope for the rotation speed of the bit of the coupled stochastic models for $\delta = 0.01$.

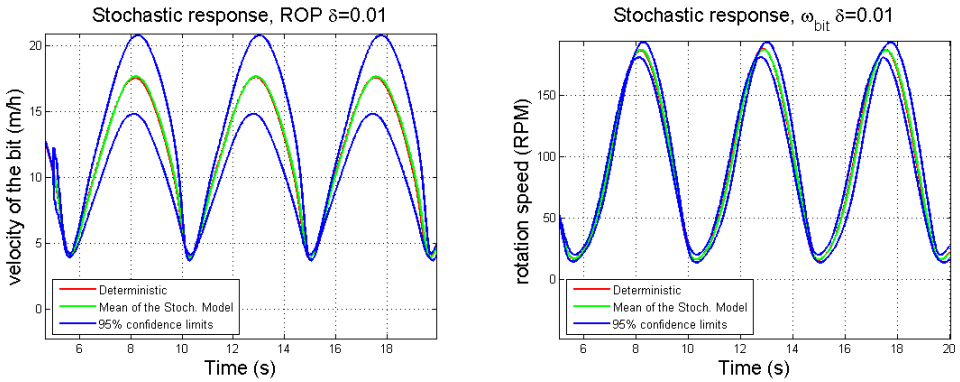

Fig. 11. Coupled stochastic model, 95% envelope. Left: rate-of-penetration, ROP. Right: rotation speed of the bit.

Note that even for $\delta = 0.01$ the stochastic response of the ROP presents a significative variance. The probability space is richer when the coupled model is used, i.e., there are more possibilities of outcome. The dispersion will be increased to verify the robustness of the bit-interaction model to model uncertainties, Fig. 12 to 13.

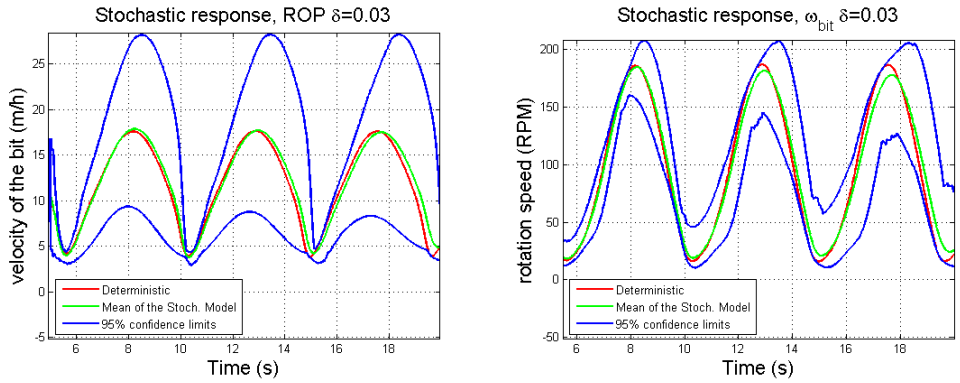

Fig. 12. Coupled stochastic model, 95% envelope. Left: rate-of-penetration, ROP. Right: rotation speed of the bit.

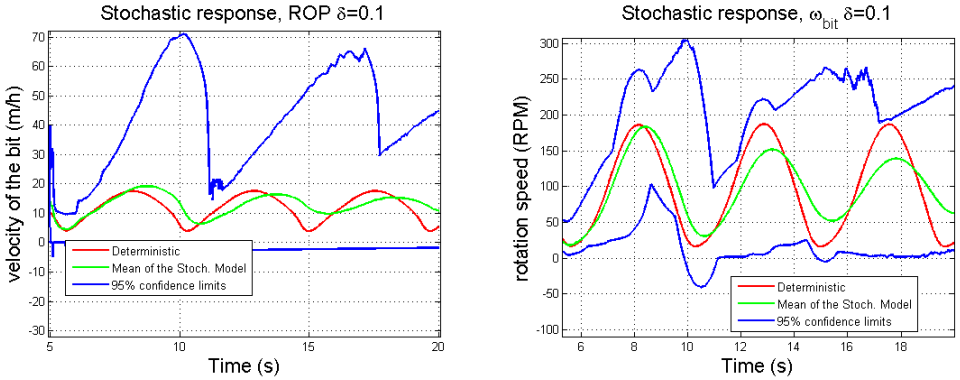

Fig. 13. Coupled stochastic model, 95% envelope. Left: rate-of-penetration, ROP. Right: rotation speed of the bit.

Fig. 13 shows that there is something that does not go right in the stochastic response of the system, take a look at the shape of the envolope. To analyze this see Fig. 14 where it is plotted 500 Monte Carlo simulations for $\delta = 0.03$.

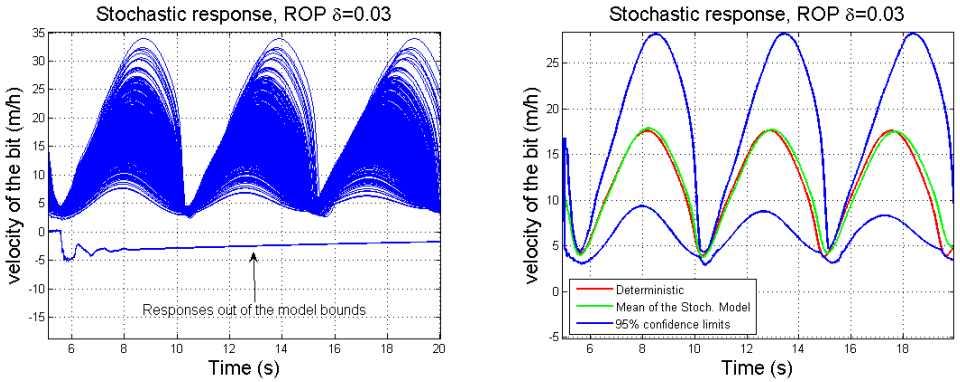

Fig. 14. Coupled stochastic model. Left: stochastic responses of the ROP. Right: 95% envelope.

Note that when the coupled stochastic model is used we are pushing the bit-rock interaction model limits: there are some realizations (the ones down in Fig. 14 left) that escape the limits of the model we are working with because the response is not close to the one that is expected for a real system. This is a good test to see the bit-rock model limits. We may say that the bit-rock interaction model, although robust to parameters change, is not robust to model uncertainties. Using the coupled stochastic model, a little perturbation in the operator responsible for the bit-rock interaction ($\delta = 0.03$) leads to a stochastic response with large confidence regions and there are some dynamic responses that do not correspond to the physics of the problem.

15 Concluding remarks

A dynamical model was developed to simulate the drill-string dynamics and it showed to be well suited. The results are coherent with the ones found in the literature, but a different model is proposed where the Timoshenko beam model is used and the main forces that influence the dynamics are considered: motor torque (as a constant rotation speed at the top), hanging force, stabilizers, bit-rock interaction that describes the rate-of-penetration ROP, shock and rubbing between the column and the borehole, fluid-structure interaction (that flows downwards then goes upwards). It was also considered a nonlinear 3D beam with finite deformations without neglecting the higher order terms and the vibration was computed about a prestressed configuration.

The fluid-structure model used have a major influence in the lateral vibration of the system. For example, if we consider only the added mass ($[M_f]$) the lateral natural frequencies decrease around 20%. If only the added stiffness ($[K_f]$) is considered, the lateral frequencies increase around 50%. In addition, the added stiffness changes the modes of the system and consequently changes the reduction basis, so the projection basis forms a different subspace in which the dynamics is represented (see a comparison of the modes with and without fluid in Fig. 3). Nevertheless the axial and torsional vibration are little affected by the fluid flow.

A reduced model is proposed where the lateral, axial, and torsional modes are chosen to compose the reduced basis. For the system analyze, if we order the modes there are two rigid body modes (axial and torsional) and then more than 100 lateral modes. The axial and torsional modes must be identified and used in the reduced basis so that the dynamics can be computed properly.

In the second part of the paper a stochastic model of the bit-rock interaction model is proposed. As the parameters of the bit-rock interaction does not correspond to parameters which can directly be identified from measurements,

it can easily be concluded that it is not really practical to use the Parametric Probabilistic Approach to model uncertainties. Then the Nonparametric Probabilistic Approach is used to take into account model uncertainties for local nonlinearities. This corresponds to a completely novel approach to take into account model uncertainties in a nonlinear constitutive equation. Since the dynamical system is globally nonlinear, an adapted strategy is developed to implement the stochastic simulation.

What is interesting is that by perturbing this operator we can investigate the limits of the bit-rock interaction model. The results showed that when no extra coupling is included in the stochastic model (i.e., when only the parameters are changed) the bit-rock interaction model is robust to uncertainties (the response is coherent with the physics of the problem and small uncertainties lead to small variance of the response), but when the extra coupling is considered (i.e., when the model is changed), a small uncertainty leads to a very spread response and there are some realizations that do not correspond to the physics of the problem. This means that this bit-rock interaction model should be used in situations close to the stable one because it was seen that the bit-rock interaction model is very sensible to model uncertainties.

References

[1] ASME. *Handbook: Drilling fluids processing.* Elsevier, Inc., 2005.

[2] K. J. Bathe. *Finite Element Procedures.* Prentice-Hall, Inc., 1996.

[3] A. Bazoune and Y.A. Khulief. Shape functions of the three-dimensional Timoshenko beam element. *Journal of Sound and Vibration*, 259(2):473–480, 2002.

[4] A. Berlioz, J. Der Hagopian, R. Dufour, and E. Draoui. Dynamic behavior of a drill-string: experimental investigation of lateral instabilities. *Journal of Vibration and Accoustics*, 118(3):292–298, 1996.

[5] C. Chen, D. Duhamel, and C. Soize. Probabilistic approach for model and data uncertainties and its experimental identification in structural dynamics: Case of composite sandwich panels. *Journal of Sound and Vibration*, 194(1-2):64–81, 2006.

[6] C. Chen, D. Duhamel, and C. Soize. Nonparametric stochastic modeling of linear systems with prescribed variance of several natural frequencies. *Probabilistic Engineering Mechanics*, 23(2-3):267–278, 2008.

[7] A. P. Christoforou and A. S. Yigit. Dynamic modeling of rotating drill-strings with borehole interactions. *Journal of Sound and Vibration*, 206(2):243–260, 1997.

[8] A. P. Christoforou and A. S. Yigit. Fully vibrations of actively controlled drillstrings. *Journal of Sound and Vibration*, 267:1029–1045, 2003.

[9] P. Coussot, F. Bertrand, and B. Herzhaft. Rheological behavior of drilling muds, characterization using MRI vizualization. *Oil and Gas Science and Technology*, 59(1):23–29, 2004.

[10] J. M. Crolet and R. Ohayon. *Computational Methods for Fluid-Structure Interaction.* John Wiley & Sons Inc., Hoboken, New Jersey, 1994.

[11] M. P. Escudier, I. W. Gouldson, P. J. Oliveira, and F. T. Pinho. Effects of inner cylinder rotation on laminar flow of a newtonian fuid through an eccentric annulus. *International Journal of Heat and Fluid Flow*, 21:92–103, 2000.

[12] M. P. Escudier, P. J. Oliveira, and F. T. Pinho. Fully developed laminar flow of purely viscous non-newtonian liquids through annuli, including the effects of eccentricity and inner-cylinder rotation. *International Journal of Heat and Fluid Flow*, 23:52–73, 2002.

[13] R. G. Ghanem and P. D. Spanos. *Stochastic Finite Elements: A Spectral Approach.* Dover Publications, Inc., Mineola, New York, 1991.

[14] T. J. R. Hughes. *The Finite Element Method - Linear Static and Dynamic Finite Element Analysis.* Prentice-Hall, Inc., Englewood Cliff, New Jersey, 1997.

[15] Y.A. Khulief and H. AL-Naser. Finite element dynamic analysis of drill-strings. *Finite Elements in Analysis and Design*, 41:1270–1288, 2005.

[16] Y.A. Khulief, F. A. Al-Sulaiman, and S. Bashmal. Vibration analysis of drillstrings with self excited stick-slip oscillations. *Journal of Sound and Vibration*, 299:540–558, 2007.

[17] S. J. Kotsonis and P. D. Spanos. Chaotic and random whirling motion of drillstrings. *Journal of Energy Resources Technology*, 119(4):217–222, 1997.

[18] M. P. Mignolet and C. Soize. Stochastic reduced order models for uncertain geometrically nonlinear dynamical systems. *Computer Methods in Applied Mechanics and Engineering*, 2008.

[19] H. D. Nelson. A finite rotating shaft element using Timoshenko been theory. *Journal of Mechanical Design*, 102:793–803, 1980.

[20] M. P. Paidoussis. *Fluid-Structure Interactions: Slender structures and Axial Flow*, volume 1. Academic Press, London, United Kingdom, 1998.

[21] M. P. Paidoussis, T. P. Luu, and S. Prabhakar. Dynamics of a long tubular cantilever conveying fluid downwards, which then flows upwards around the cantilever as a confined annular flow. *Journal of Fluids and Structures*, 2007.

[22] John G. Papastravridis. *Analytical Mechanics*. Oxford University Press, New York, N.Y, USA, 2002.

[23] E. P. F. Pina and M. S. Carvalho. Three-dimensional flow of a newtonian liquid through an annular space with axially varying eccentricity. *Journal of Fluids Engineering*, 128(2):223–231, 2005.

[24] M. T. Piovan and R. Sampaio. On linear model for coupled axial/torsional/flexural vibrations of drill-strings. *Third European Conference on Computational Mechanics: Solids, Structures and Coupled Problems in Engineering, Lisboa, Portugal*, 2006.

[25] J. N. Reddy. *An Introduction to the Finite Element Method*. McGraw-Hill, 2005.

[26] R. M. Rosenberg. *Analytical Dynamics*. Plenum Press, New York, USA, 1980.

[27] R. Sampaio and S. Bellizzi. POMs analysis obtained from Karhunen-Loève expansion for randomly vibrating systems. *Journal of Sound and Vibration*.

[28] R. Sampaio, M. T. Piovan, and G. V. Lozano. Coupled axial/torsional vibrations of drilling-strings by mean of nonlinear model. *Mechanics Research Comunications*, 34(5-6):497–502, 2007.

[29] R. Sampaio and C. Soize. On measures of nonlinearity effects for uncertain dynamical systems - application to a vibro-impact system. *Journal of Sound and Vibration*, 303:659–674, 2007.

[30] R. J. Serfling. *Approximation Theorems of Mathematical Statistics*. John Wiley and Sons, USA, 1980.

[31] C. E. Shannon. A mathematical theory of communication. *Bell System Tech. J.*, 27:379–423 and 623–659, 1948.

[32] C. Soize. A nonparametric model of random uncertities for reduced matrix models in structural dynamics. *Probabilistic Engineering Mechanics*, 15:277–294, 2000.

[33] C. Soize. Maximum entropy approach for modeling random uncertainties in trasient elastodynamics. *Journal of the Acoustical Society of America*,

109(5):1979–1996, 2001.
[34] C. Soize. Transient responses of dynamical systems with random uncertainties. *Probabilistic Engineering Mechanics*, 16(4):363–372, 2001.
[35] C. Soize. A comprehensive overview of a non-parametric probabilistic approach of model uncertainties for predictive models in structural dynamics. *Journal of Sound and Vibration*, 288(3):623–652, 2005.
[36] C. Soize. Random matrix theory for modeling uncertainties in computational mechanics. *Computer Methods in Applied Mechanics and Engineering*, 194(12-16):1333–1366, 2005.
[37] P. D. Spanos and A. M. Chevallier. Non linear stochastic drill–string vibrations. In *8th ASCE Specialty Conference on Probabilistic Mechanics and Structural Reliability*, 2000.
[38] P. D. Spanos, A. K. Sengupta, R. A. Cunningham, and P. R. Paslay. Modeling of roller cone bit lift-off dynamics in rotary drilling. *Journal of Energy Resources Technology*, 117(3):197–207, 1995.
[39] M. A. Trindade, C. Wolter, and R. Sampaio. Karhunen–Loève decomposition of coupled axial/bending of beams subjected to impacts. *Journal of Sound and Vibration*, 279:1015–1036, 2005.
[40] R. W. Tucker and C. Wang. An integrated model for drill-string dynamics. *Journal of Sound and Vibration*, 224(1):123–165, 1999.
[41] R. W. Tucker and C. Wang. Torsional vibration control and cosserat dynamics of a drill-rig assembly. *Meccanica*, 38(1):143–159, 2003.
[42] A. Yigit and A. Christoforou. Coupled axial and transverse vibrations of oilwell drillstrings. *Journal of Sound and Vibration*, 195(4):617–627, 1996.

A Data used in the simulation

$L_{dp} = 1400$ [m] (length of the drill pipe), $L_{dc} = 200$ [m] (length of the drill collar), $D_{odp} = .127$ [m] (outside diameter of the drill pipe), $D_{odc} = .2286$ [m] (outside diameter of the drill collar), $D_{idp} = .095$ [m] (inside diameter of the drill pipe), $D_{idc} = 0.0762$ [m] (inside diameter of the drill collar), $D_{ch} = 0.3$ [m] (diameter of the borehole (channel)), $x_{stab} = 1400$ [m] (location of the stabilizer), $k_{stab} = 17.5$ [MN/m] (stiffness of the stabilizer per meter), $E = 210$ [GPa] (elasticity modulus of the drill string material), $\rho = 7850$ [kg/m^3] (density of the drill string material), $\nu = .29$ [-] (poisson coefficient of the drill string material), $k_s = 6/7$ [-] (shearing correcting factor), $c_1 = 0.05$ [N.s/m] (friction coefficient for the axial rigid body motion), $c_2 = 0.05$ [N.s/m] (friction coefficient for the rotation rigid body motion), $\xi_i = 0.3$ [-] i-th (damping factor), $k_{sh} = 1e8$ [N/m] (stiffness per meter used for the shocks), $\mu_{sh} = 0.0005$ [-] (friction coefficient between the string and the borehole), $\Omega_x = 100$ [RPM] (constant speed at the top), $U_i = 1.5$ [m/s] (flow velocity in

the inlet), $\rho_f = 1200$ [kg/m^3] (density of the fluid), $C_f = .0125$ [-] (fluid viscous damping coefficient), $k = 0$ [-] (fluid viscous damping coefficient), $wob = 100$ [kN] (initial weight on the bit), $g = 9.81$ [m/s^2] (gravity acceleration), $a_1 = 3.429e-3$ [m/s] (constant of the bit-rock interaction model), $a_2 = 5.672e-8$ [m/(N.s)] (constant of the bit-rock interaction model), $a_3 = 1.374e-4$ [m/rd] (constant of the bit-rock interaction model), $a_4 = 9.537e6$ [N.rd] (constant of the bit-rock interaction model), $a_5 = 1.475e3$ [N.m] (constant of the bit-rock interaction model), $e = 2$ [rd/s] (regularization parameter).